





SUPPLEMENTARY MATERIALS

Bioactive Chitosan/ β -Tricalcium Phosphate Coatings on Titanium: Experimental Optimization and DFT Insight

Rakiya Yu. Milusheva¹, Ilmar N. Nurgaliev^{1*},
Akmal B. Abilkasimov², Sayora Sh. Rashidova¹

¹Institute of Polymer Chemistry and Physics of the Academy of Sciences of the Republic of Uzbekistan, Tashkent, Uzbekistan;

²Kimyo International University in Tashkent, Tashkent, Uzbekistan

(*Corresponding author's e-mail: ilnarvodnik@gmail.com)

List of Content

Figure S1. FTIR spectrum of purified chitosan <i>Bombyx mori</i> with $M_V = 113$ kDa.	S1
Figure S2. (a) IR spectrum; (b) X-ray diffraction pattern of $\text{Ca}_3(\text{PO}_4)_2$	S2
Figure S3. Images of processed titanium plates with different roughness: (a) Original titanium plate, plate roughness $1.66\ \mu\text{m}$; (b) Primary processing - plate roughness $2.58\ \mu\text{m}$; (c) Final processing - plate roughness - $4.09\ \mu\text{m}$. Schematic diagram of the installation for electrolytic deposition of coatings on titanium plates.	S3
Figure S4. (a) Spectrum of the titanium plate; (b) Spectrum of TCP — $\text{Ca}_3(\text{PO}_4)_2$; (c) Spectrum of CS-BM.	S4
Table S1. Adsorption energies, key interaction motifs, and estimated charge transfer values (in electrons) for individual and combined bioactive components adsorbed on the $\text{TiO}_2(110)$ surface.	S5
Figure S5. Adsorption energy diagram for individual and combined bioactive components adsorbed on the $\text{TiO}_2(110)$ surface	S6
Figure S4. Electrostatic potential (ESP) map of the rutile $\text{TiO}_2(110)$ surface, illustrating the spatial distribution of positive and negative charge regions. These charge patterns highlight potential adsorption sites and interactions with chitosan molecules and phosphate species, providing insight into the interfacial binding behavior.	S7

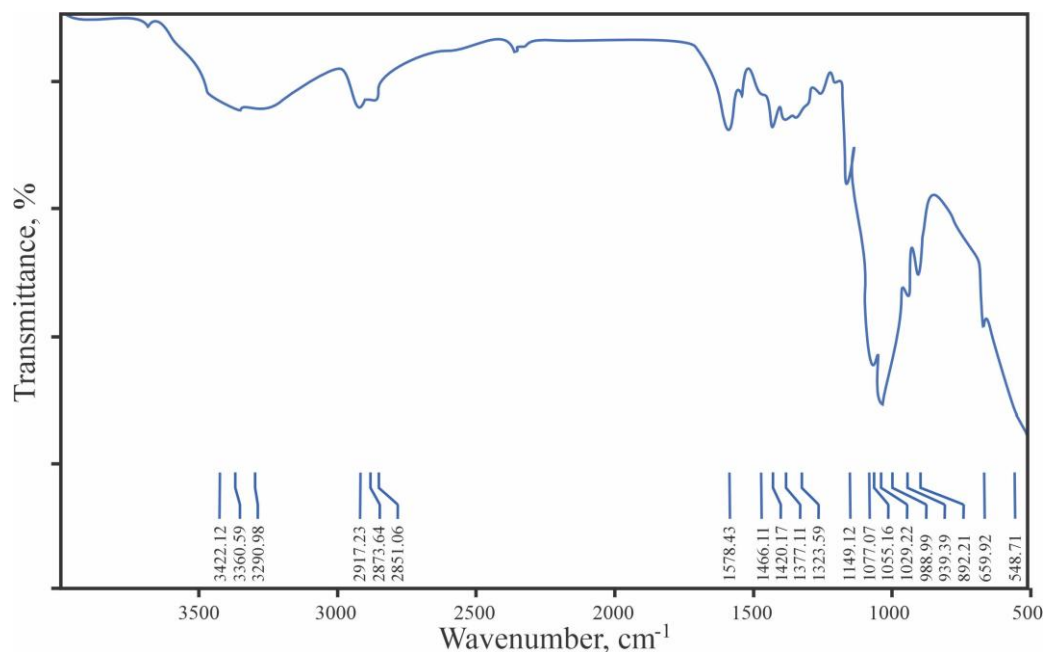


Figure S1. FTIR spectrum of purified chitosan *Bombyx mori* with $M_V = 113$ kDa.

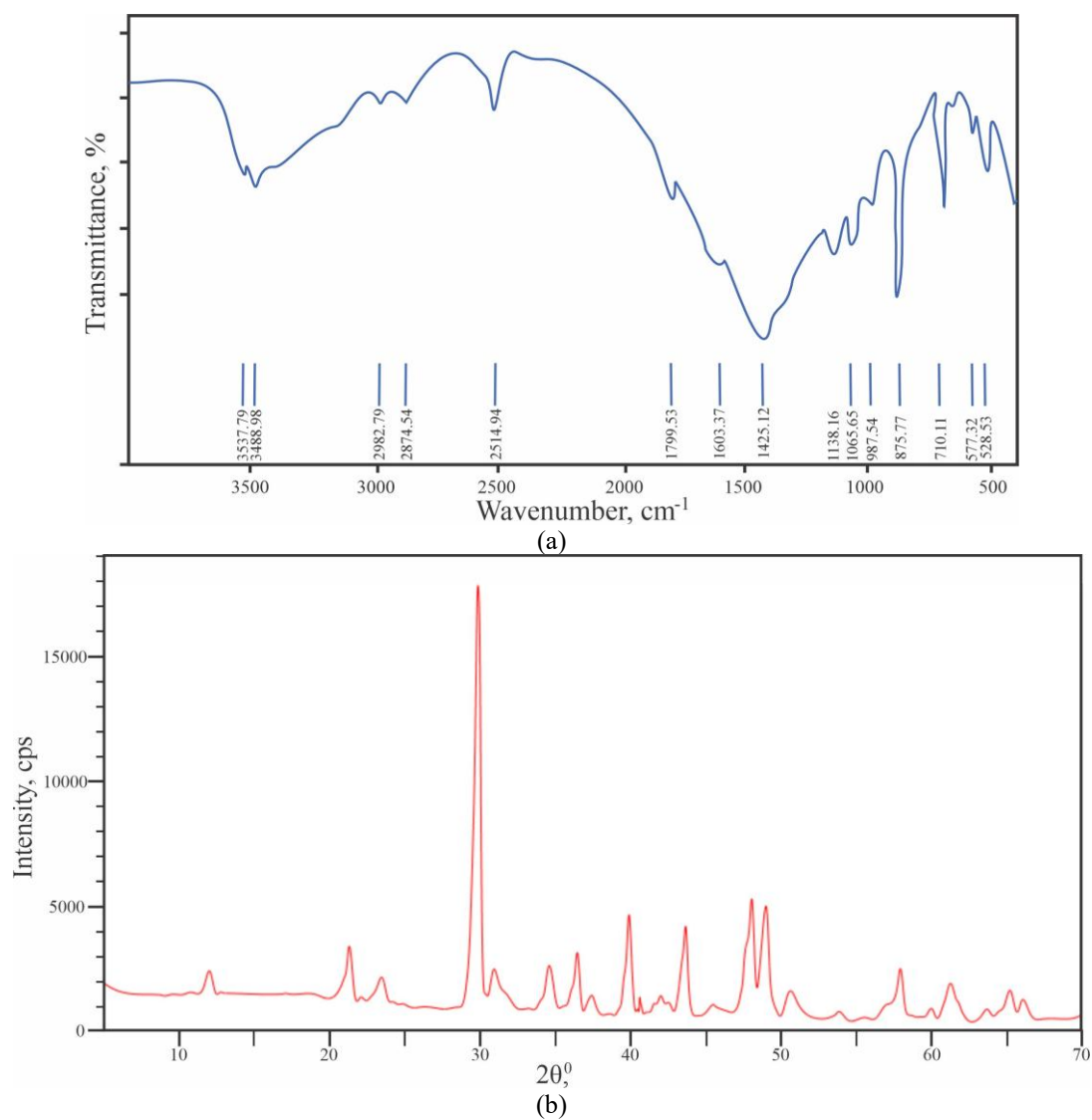
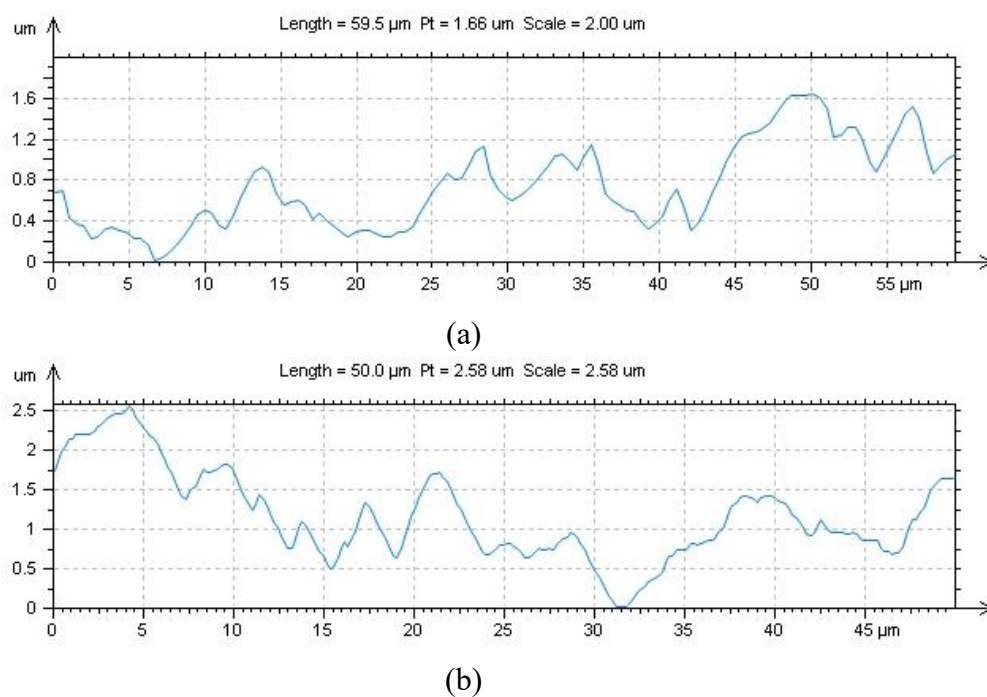
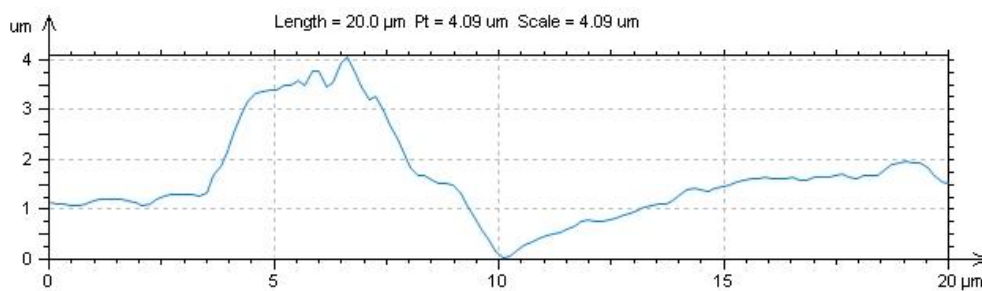


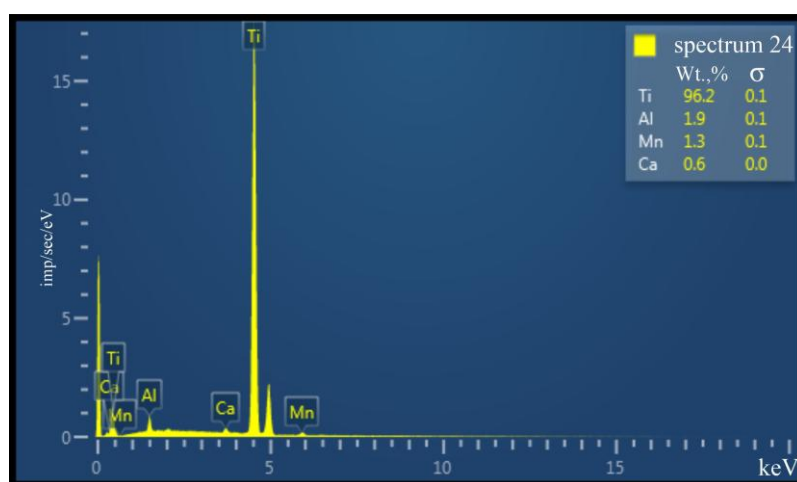
Figure S2. (a) IR spectrum; (b) X-ray diffraction pattern of TCP — $\text{Ca}_3(\text{PO}_4)_2$



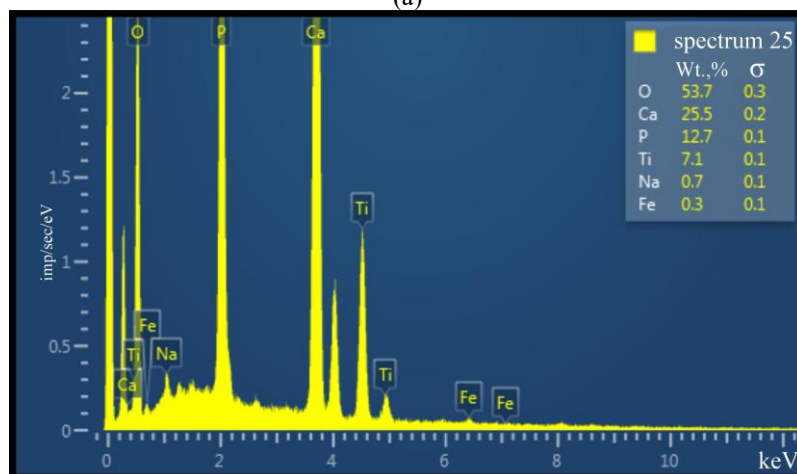


(c)

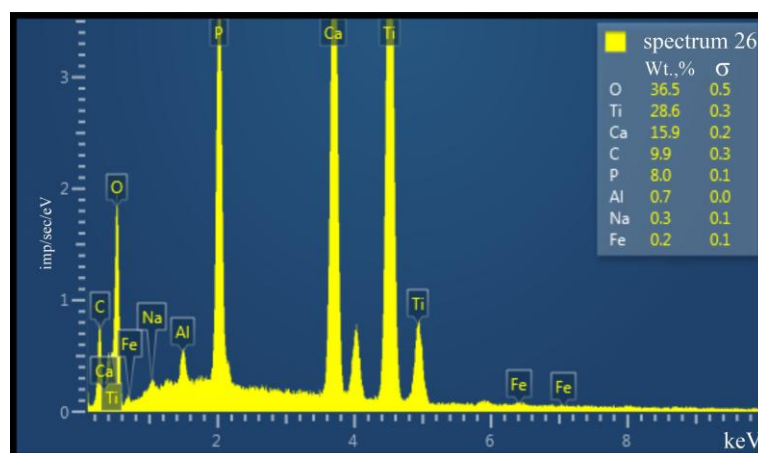
Figure S3. Images of processed titanium plates with different roughness: (a) Original titanium plate, plate roughness 1.66 μm ; (b) Primary processing - plate roughness 2.58 μm ; (c) Final processing - plate roughness - 4.09 μm . Schematic diagram of the installation for electrolytic deposition of coatings on titanium plates.



(a)



(b)



(c)

Figure S4. (a) Spectrum of the titanium plate; (b) Spectrum of TCP — $\text{Ca}_3(\text{PO}_4)_2$; (c) Spectrum of CS-BM.

Table S 1

Adsorption energies, key interaction motifs, and estimated charge transfer values (in electrons) for individual and combined bioactive components adsorbed on the $\text{TiO}_2(110)$ surface.

Adsorbate	Adsorption Energy, eV	Key Interactions	Charge Transfer, e^-
Glucosamine $[\text{GlcNH}_3]^+$	-1.27	NH_3^+-O , $\text{OH}-\text{Ti}^{5c}$	0.11
Ca^{2+}	-1.85	$\text{Ca}-\text{O} (\times 3)$	0.00
PO_4^{3-}	-1.43	$\text{P}-\text{O}-\text{Ti} (\times 3)$	0.21
$\text{CS}-\text{Ca}^{2+}-\text{PO}_4^{3-}$	-3.62	Multisite (cooperative)	0.25 (total)

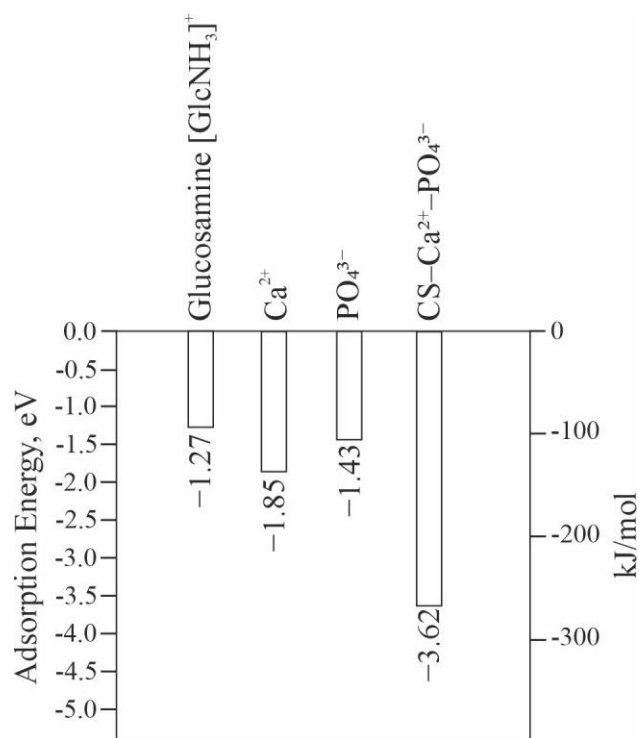


Figure S5. Adsorption energy diagram for individual and combined bioactive components adsorbed on the $\text{TiO}_2(110)$ surface

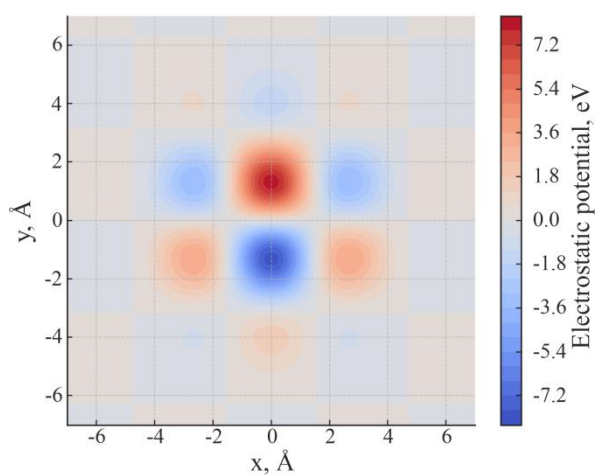


Figure S6. Electrostatic potential (ESP) map of the rutile $\text{TiO}_2(110)$ surface, illustrating the spatial distribution of positive and negative charge regions. These charge patterns highlight potential adsorption sites and interactions with chitosan molecules and phosphate species, providing insight into the interfacial binding behavior.